First-principles analysis of the structural, electronic, and elastic properties of cubic organic–inorganic perovskite $HC(NH_2)_2PbI_3$*

Jun-Fei Wang(王俊斐)†, Xiao-Nan Fu(富笑男), and Jun-Tao Wang(王俊涛)

College of Science, Henan University of Technology, Zhengzhou 450001, *China*

(Received 2 April 2017; revised manuscript received 20 June 2017; published online 20 August 2017)

The structural, electronic, and elastic properties of cubic $HC(NH_2)_2PbI_3$ perovskite are investigated by density functional theory using the Tkatchenko–Scheffler pairwise dispersion scheme. Our relaxed lattice parameters are in agreement with experimental data. The hydrogen bonding between NH_2 and I ions is found to have a crucial role in $FAPbI_3$ stability. The first calculated band structure shows that $HC(NH_2)_2PbI_3$ has a direct bandgap (1.02 eV) at *R*-point, lower than the bandgap (1.53 eV) of $CH_3NH_3PbI_3$. The calculated density of states reveals that the strong hybridization of s(Pb)–p(I) orbital in valence band maximum plays an important role in the structural stability. The photo-generated effective electron mass and hole mass at *R*-point along the *R*–Γ and *R*–*M* directions are estimated to be smaller: $m_e^* = 0.06m_0$ and $m_h^* = 0.08m_0$ respectively, which are consistent with the values experimentally observed from long range photocarrier transport. The elastic properties are also investigated for the first time, which shows that $HC(NH_2)_2PbI_3$ is mechanically stable and ductile and has weaker strength of the average chemical bond. This work sheds light on the understanding of applications of $HC(NH_2)_2PbI_3$ as the perovskite in a planar-heterojunction solar cell light absorber fabricated on flexible polymer substrates.

Keywords: first-principles, electronic structure, charge carrier mobility, elastic properties

PACS: 63.20.dk, 74.25.Jb, 72.20.Jv, 71.15.Mb **DOI:** 10.1088/1674-1056/26/10/106301

1. Introduction

Methylammonium lead trihalide perovskite $CH_3NH_3Pbl_3$ ($MAPbl_3$) or $MAPbl_3$-based photovoltaic solar cells have demonstrated recorded power conversion efficiency (PCE) as high as 21.0%.[1] The superb photovoltaic performances of $MAPbl_3$ originate from its high absorption coefficient, good electrical transport properties, and favorable band gap (1.55 eV).[2–5] However, at solar cell operating temperature (> 300 K), $MAPbl_3$ will undergo reversible structure phase transition, causing its band structure to change,[5] which can importantly affect the photovoltaic properties. The better thermal stability and low-bandgap of perovskites are required in order to further improve the PCE.

In recent investigations, formamidinium-based perovskite $HC(NH_2)_2PbI_3$ ($FAPbI_3$) solar cells have come into being as a promising alternative to $MAPbl_3$-based perovskite solar cells,[6–11] due to the better thermal stability, lower bandgap, and wider absorption range.[6,11] In 2014, Lee *et al.* reported that $FAPbI_3$ coupled with a mesoporous TiO_2 layer reached about 16% PCE via a two-step deposition procedure.[11] In 2015, a maximum PCE as high as 20.1% from solar cells based on $FAPbI_3$ was demonstrated.[12] In 2016, Bi *et al.* reported that the PCE reached 20.6% by using $FAPbI_3$ as an absorption layer.[13] Despite the rapid increase in $FAPbI_3$ the solar cell efficiency is related to the device evolution. However, most of the fundamental physical properties of $FAPbI_3$ have not yet been well studied.

According to the previous research,[14] dry crystals of black $FAPbI_3$ (α-phase) are found to be converted into β-phase below 200 K and γ-phase below 130 K, which indicates that the α-phase has excellent stability above room temperature. The black α-phase of $FAPbI_3$ perovskite was found to possess a cubic perovskite unit cell in high resolution neutron powder diffraction experiment in 2015.[15] The α-phase is the necessary and most important phase for the $FAPbI_3$ perovskite solar cell application. However, the electronic and elastic properties of α-$FAPbI_3$ have not yet been well investigated. Hence, it is necessary to investigate the structural, electronic and elastic properties of cubic $FAPbI_3$ by first-principles studies.

2. Computational details

The density function theory (DFT) calculations are performed by using the Vienna *ab initio* simulation package (VASP) code.[16] The projector augmented-wave (PAW) pseudopotentials[17] are used with an energy cutoff of 500 eV for the plane-wave basis functions. Electronic orbitals 5d6s6p, 5s5p, 2s2p, 2s2p, and 1s are considered in valence for Pb, I,

*Project supported by the National Natural Science Foundation of China (Grant No. 51572219), the Natural Science Foundation of Shaanxi Province, China (Grant No. 2015JM1018), the Graduate Innovation Fund of Northwest University of China (Grant No. YJG15007), the Henan Provincial Foundation and Frontier Technology Research Program, China (Grant Nos. 2013JCYJ12 and 2013JCYJ13), the Fund from Henan University of Technology, China (Grant No. 2014YWQN08), and the Natural Science Fund from the Henan Provincial Education Department, China (Grant No. 16A140027).

†Corresponding author. E-mail: junfei_w@126.com

© 2017 Chinese Physical Society and IOP Publishing Ltd

C, N, and H atoms, respectively. The Monkhorst–Pack scheme with a $4\times4\times4$ k-mesh[18] is employed for structural and electronic calculations, $8\times8\times8$ k-mesh is adopted for the elastic analysis. Further increasing the energy cutoff and k-points show little difference in result. All the structures considered in this study are relaxed with a conjugate-gradient algorithm until the energy on the atoms is less than 1.0×10^{-4} eV.

For the exchange–correlation functional, the generalized gradient approximation (GGA) of Perdew–Burke–Ernzerhof (PBE)[19] is used. The van der Waal's interaction (vdW) between the organic cation and the inorganic ion is calculated by employing the Tkatchenko–Scheffler (TS) pairwise dispersion scheme.[20] Accordingly, the calculations incorporating TS-vdW are labelled by "PBE+TS" hereafter.

3. Results and discussion

3.1. Structure

It has been shown in previous DFT calculations that certain molecular orientations can affect the corresponding Pb–I inorganic frame and thus change the stability of the material.[21] For the cubic $MAPbI_3$ structure, we should note that there are three local minima when the MA dipole is aligned along the [100], [110], and [111] directions respectively.[22] Therefore, in order to analyze in detail the stability of $FAPbI_3$, we consider the above three orientations of the FA dipole. The calculated total energies are −47.8562 eV ([100] orientation), −47.8137 eV ([110] orientation), and −47.7316 eV ([111] orientation) respectively, which shows that the cubic FAPbI3 structure with FA aligned along the [100] direction has the smallest total energy and is most stable.

The most stable relaxed cubic $FAPbI_3$ structure is obtained by using the PBE+TS method and shown in Fig. 1. In the unit cell of a bulk cubic $FAPbI_3$ (Fig. 1), each Pb atom is surrounded by six I atoms, of which four I atoms are in the equatorial direction and two I atoms in the apical direction. The organic formamidinium ion is embedded in the octahedron PbI_6 cage. The orientation for the triangular-planar formamidinium cation in the unit cell midplane is that the orientation of the C–H bond identified is the y direction with weaker CH$\cdots$I interactions (3.573 Å), and the orientation for the N–C–N plane is in the xy plane for the potential formation of weak NH$\cdots$I hydrogen bonds (2.763 Å and 2.984 Å). The Pb–I bond length is 3.177 Å. The calculated results above show that the main interaction between the organic cations and inorganic framework is through the ionic bonding between NH_2 and I ions. Fully relaxed lattice constant ($a=6.353$ Å) and atomic coordinates are listed in Table 1, which are in excellent agreement with the experimental data.[15] According to Table 1, if vdW force is included in the relaxation, the discrepancy between the calculated result and the experimental value will become $<2\%$, that is, the crystal structure is properly described. Moreover, NH_2CHNH_2 and CH_3NH_3 have similar sizes, so the equilibrium lattice constants of cubic $FAPbI_3$ and $MAPbI_3$ phase ($a=6.329$ Å)[23] are nearly the same.

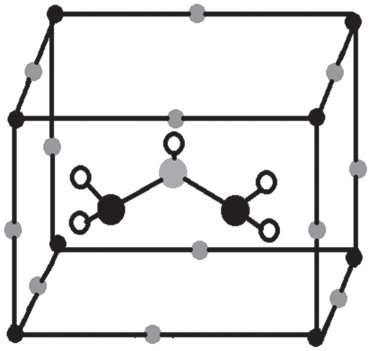


Fig. 1. Unit cell structure of cubic $HC(NH_2)_2PbI_3$, with small black balls representing Pb atoms, small gray balls the I atoms, big gray balls the C atoms, big black balls the N atoms, and small empty black balls the H atoms.

Table 1. Space group (SG), values of equilibrium lattice constant a (Å) and volume V (Å^3 atom), atomic positions of Pb, I, C, N, and H atoms of calculated cubic $FAPbI_3$.

	This work	Ref. [15]
SG	*Pm3m*	*Pm3m*
a	6.353	6.362
V	256.411	257.502
Atomic position of Pb	(0.0,0.0,0.0)	(0.0,0.0,0.0)
Atomic position of I	(0.5,0.0,0.0)	(0.5, 0.0, 0.0)
Atomic position of C	(0.5,0.5763,0.5)	(0.5,0.5726,0.5)
Atomic position of N	(0.6842,0.4793,0.5)	(0.6820,0.4781,0.5)
Atomic position of H	(0.5, 0.7534, 0.5)	(0.5, 0.7447, 0.5)
	(0.8158, 0.5747, 0.5)	(0.8142, 0.5680, 0.5)
	(0.7046,0.3149,0.5)	(0.7025,0.3179,0.5)

3.2. Electronic properties

According to the relaxed cubic structure, we investigate the electronic properties of $FAPbI_3$, which are shown in Figs. 2(a) and 3(a)–3(d). Moreover, in order to compare the band structure of tetragonal $MAPbI_3$ with the bandgap of $FAPbI_3$, we also calculate the band structure of tetragonal $MAPbI_3$ as shown in Fig. 2(b). Figures 2(a) and 2(b) show that the valence-band maximum (VBM) values and conduction-band minimum (CBM) values located respectively at the R (0.5, 0.5, 0.5) point for $FAPbI_3$ and Γ (0.0, 0.0, 0.0) point for $MAPbI_3$, indicating that they are direct gap semiconductors. The calculated bandgap of $FAPbI_3$ at R point is 1.02 eV, significantly underestimated compared with the experimental value of 1.43 eV,[9] and for $MAPbI_3$, the bandgap on Γ point is 1.53 eV, very close to the experimental value (1.55 eV).[4,5] Their different bandgaps indicate that the bandgap is greatly affected by not only the phases but also the cation size and distribution of organic cation (FA^+ and MA^+). The obtained bandgap on R point of $FAPbI_3$ is smaller than that of $MAPbI_3$

and allowed for near-infrared absorption, so the $FAPbI_3$ is superior to $MAPbI_3$ to serve as a light harvester, which is consistent with experimental result.[4] The calculated band structure of $MAPbI_3$ is found to be very similar to a previously reported result,[24] which indicates that our calculated band structures are reasonable.

Because the projected density of states (PDOS) and the total density of states (TDOS) provide an in-depth insight into the electronic properties.[25] The PDOS and TDOS for $FAPbI_3$ are presented in Figs. 3(a)–3(d). As seen in Fig. 3, the VBM is comprised of the antibonding combination of Pb 6s orbitals and 5p orbits of I, and the CBM is composed of 6p-orbitals of Pb. Also, it is found that the organic cation FA^+ is far from the Fermi level, so that the FA cation plays only the role of an electron donor in the system. Therefore, the reason for the emergency of the photocurrent is explained by the electron transition from 5p orbitals of I and 5s orbital of Pb to the 5p orbitals of Pb. The calculated results also clearly suggest that the interaction between organic cation and the inorganic matrix greatly affects the structure, which, in turn, changes the electronic structure of $FAPbI_3$.

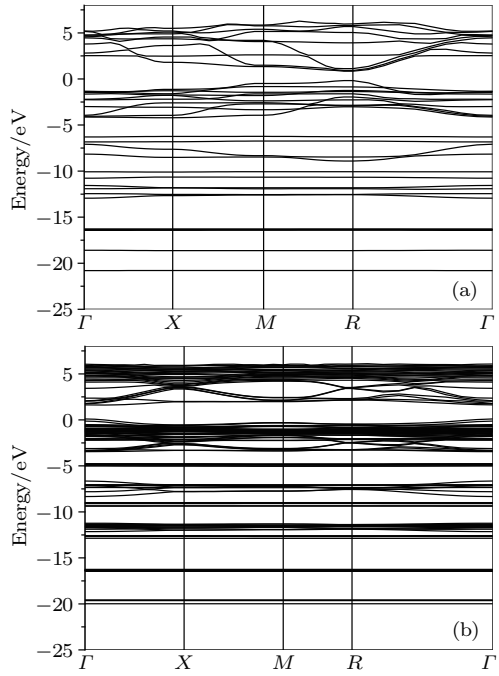


Fig. 2. Calculated band structures of (a) cubic $FAPbI_3$ and (b) tetragonal $MAPbI_3$ between high symmetry points.

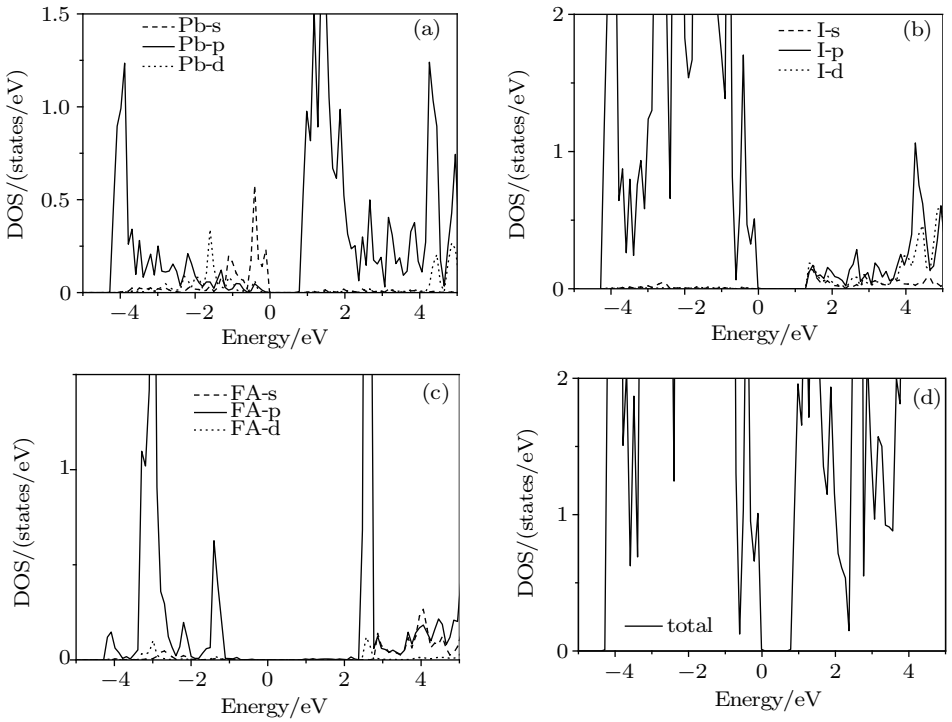


Fig. 3. Calculated ((a)–(c)) PDOS and (d) TDOS of cubic $FAPbI_3$ perovskite.

Considering the fact that the photoelectric activity of photovoltaic material $FAPbI_3$ is related to the mobilities of photogenerated electrons and holes, the mobility of photo-excited carriers (electrons and holes) can be indirectly estimated by their effective mass. Here, we calculate the effective mass of electrons (m_e^*) around CBM and holes (m_h^*) at VBM of $FAPbI_3$ according to the following relation:[21]

$$m^* = \hbar^2 \left[\frac{\partial^2 E(k)}{\partial k^2} \right]^{-1}, \tag{1}$$

where m^* is the effective mass of electrons or holes, $\hbar$ the reduced Planck constant, $E(k)$ the band edge eigenvalue, and k the wave vector. For cubic $FAPbI_3$, by fitting the function, the m_e^* and m_h^* along the R–Γ and R–M direction at CBM and VBM (in Fig. 2(a)) are first obtained to be $0.06m_0$ and

$0.08m_0$ respectively, which are in good agreement with recent predictions ($m^* = 0.09$–$0.1m_0$) from Galkowski *et al.*[26] However, the obtained m_e^* and m_h^* are smaller than the estimated values ($m_e^* > 0.22m_0$ and $m_h^* > 0.14m_0$) of m_e^* and m_h^* of $CH_3NH_3PbX_3$ and $CsPbX_3$ (X = Cl, Br, and I).[27] The calculated m_e^* and m_h^* above confirm that the $FAPbI_3$ has lighter electrons or holes, showing that the photo-excited carriers have high mobility or excellent transport rate. The obtained different effective electron and hole mass are in good accordance with experimentally measured diffusion coefficients for electron (0.004 ± 0.001 $cm^2 \cdot s^{-1}$) and hole (0.091 ± 0.009 $cm^2 \cdot s^{-1}$), so are the diffusion lengths for electrons (177 ± 20 nm) and for holes (813 ± 72 nm).[28] These results are also consistent with the experimentally observed long range photocarrier transport results in $FAPbI_3$.[29] Owing to our obtained reasonable band structures, it is believed that the effective mass values of electrons and holes are considered as more reliable results.

3.3. Elastic properties

The crystallinity and stress state of the perovskite layer can strongly affect the absorption performances of perovskite solar cell, and the elastic properties of perovskite layer material contribute to revealing its strain, stress, fracture mechanics, and deformation. So it is necessary to analyze the elastic properties of perovskite in the system for practical applications.[30] To the best of our knowledge, the calculations of elastic properties for our $FAPbI_3$ system have not been reported so far.

To investigate the elastic properties of the $FAPbI_3$, it is critical to first analyze the stability of $FAPbI_3$ at a finite temperature. Theoretically, the phase stability at finite temperature is determined by comparing the free energies of phases. The free energy (F) can be expressed as

$$F = U - TS, \tag{2}$$

where U is the internal energy of the phase. T and S are the temperature and entropy of the phase respectively. To obtain the F of $FAPbI_3$ at a finite temperature, we approximately calculate the average entropies of the system using the above three different orientations of the FA dipole by calculating their phonon spectra. The obtained average entropies are 0.688 meV ([100] orientation), 0.832 meV ([110] orientation), and 0.965 meV ([111] orientation) respectively. According to the total energies (or the internal energy) obtained above, we calculate the free energies of the system with three different orientations of the molecule between 0 K and 1000 K in steps of 100 K by using Eq. (2). The F calculation results show that the $FAPbI_3$ with [100] orientation has the smallest F in the whole temperature range, which implies that it is the most stable in the whole temperature range. Hence, the elastic properties of the $FAPbI_3$ phase with [100] orientation will be investigated.

The elastic properties describe the mechanic properties of materials under the strain. The elastic constants C_{ij} are obtained by calculating the total energy as a function of volume conserving strains through using the Mehl method.[31] Only three independent elastic constants (C_{11}, C_{12}, and C_{44}) are required in order to describe a cubic structure, and the parameterizations of three strains used to calculate three elastic constants of cubic are shown in Ref. [32] Our calculated three elastic constants are shown in Table 2, i.e., $C_{11} = 20.5$ GPa, $C_{12} = 12.3$ GPa, and $C_{44} = 4.8$ GPa, which fulfil the mechanical stability conditions of cubic system [$(C_{11} + 2C_{12}) > 0$, $C_{44} > 0$, $C_{11} > 0$, $(C_{11} - C_{12}) > 0$].[33] Moreover, C_{11}, C_{12}, and C_{44} represent the uniaxial deformation along the [001], [010], and [100] direction, respectively. The calculated C_{44} is the smallest value, showing that there is a weak resistance to shear in the (100) plane. According to the obtained elastic constants, the other interesting elastic properties for applications such as elastic anisotropic factor (A), bulk modulus (B), shear modulus (G), Young's modulus (E), and Poisson's ratio (ν) can be obtained from the following relations:[33,34]

$$A = \frac{2C_{44}}{C_{11}-C_{12}}, \quad B = \frac{C_{11}+2C_{12}}{3}, \quad G = \frac{G_V+G_R}{2},$$
$$E = \frac{9BG}{3B+G}, \quad \nu = \frac{3B-2G}{2(3B+G)}, \tag{3}$$

where G_V is the Voigt's shear modulus and G_R is the Reuss's shear modulus. They can be expressed as[33]

$$G_V = \frac{C_{11}-C_{12}+C_{44}}{5}, \quad \frac{5}{G_R} = \frac{4}{C_{11}-C_{12}} + \frac{3}{C_{44}}. \tag{4}$$

The above calculation results are also presented in Table 2. For an isotropic crystal, the factor A must be equal to unity, while any value different from unity is a measure of elastic anisotropy degree possessed by the crystal.[35] As can be seen from Table 2, the value of elastic anisotropic factor for cubic $FAPbI_3$ structure is close to 1.0, which means that the cubic $FAPbI_3$ is stable in ambient condition, which is in accordance with the experimental result.[6,11] A ratio of B/G is usually used to differentiate between the ductile and brittle character of material.[36] Our calculated B/G (4.3) is larger than the critical value 1.75, implying that the cubic $FAPbI_3$ has a ductile nature and is subjected to bending, tensile and compression, which originates from the vdW among the FA^+ cation and the inorganic ions. The E of a material is the usual property used to characterize stiffness.[37] The higher the value of E, the stiffer the material is. The E of $FAPbI_3$ is 9.9 GPa smaller than the E (12.8 GPa) of $MAPbI_3$,[38] which indicates that $FAPbI_3$ is softer than the $MAPbI_3$. The structure with Poisson's ratio (> 0.26) suggests that it has a ductile nature. The calculated Poisson's ratio is larger than 0.3 for our structure, which indicates that the cubic $FAPbI_3$ is ductile, which is in accordance with the conclusion from the E value.

Table 2. Values of elastic constant C_{ij} (GPa), elastic anisotropic factor A, bulk modulus B (GPa), shear modulus G (GPa), B/G, Young's modulus E (GPa), Poisson's ratio ν, transverse velocity v_t (m/s); longitudinal velocity v_l (m/s), sound velocity v_m (m/s), Debye temperature v_D (K).

	C_{11}	C_{12}	C_{44}	A	B	G	B/G	E	ν	v_t	v_l	v_m	θ_D
Cubic-$FAPbI_3$	20.5	4.8	12.3	1.2	15.3	3.6	4.3	9.9	0.4	1259	2374	1407	110

The Debye temperature θ_D is also closely related to the elastic properties. According to the calculated elastic constants, we can proceed with estimating the sound velocities and the θ_D from the following equation:[39]

$$\theta_D = \frac{h}{k}\left(\frac{3}{4\pi v_\alpha}\right)^{1/3} v_m, \tag{5}$$

where h, k, v_α, and v_m are the Planck's constant, Boltzmann's constant, atomic volume, and sound velocity respectively. For In polycrystalline material, the average sound velocity is given by[39]

$$v_m = \left[\frac{1}{3}\left(\frac{2}{v_t^3}+\frac{1}{v_l^3}\right)\right]^{-1/3}, \tag{6}$$

where v_t and v_l are the transverse and the longitudinal velocity in the polycrystalline material respectively, which are given by the following relations.[40]

$$v_t = \left(\frac{G}{\rho}\right)^{1/2}, \quad v_l = \left(\frac{3B+4G}{3\rho}\right)^{1/2}. \tag{7}$$

The calculated values of v_t, v_l, and θ_D of cubic $FAPbI_3$ are also shown in Table 2. The calculated θ_D is 110 K, lower than the obtained Debye temperatures of $CH_3NH_3PbX_3$ (X = Br, I),[36] which indicates that the cubic $FAPbI_3$ with the larger FA^+ cation has a weaker strength of the average chemical bond.

4. Conclusions

The structural, electronic, and elastic properties of cubic $HC(NH_2)_2PbI_3$ perovskite are studied by the first principle calculations using PBE+TS scheme. The optimized structure is in accordance with the experimental result. The main interaction between the organic cations and inorganic framework is through the ionic bonding between NH_2 and I ions. The calculated bandgap of $FAPbI_3$ at R point is smaller than that of $MAPbI_3$, which accords with the experimental result. The further analyses of obtained TDOS and PDOS reveal that the VBM of an anti-bonding Pb s/I p combination is formed, while the CBM of empty Pb p orbitals is formed. We estimate the effective electron and hole mass values of photocarriers in FAPbI3 to be $m_e^* = 0.06m_0$ and $m_h^* = 0.08m_0$ respectively, which are very close to the measured values near $0.09m_0$. The obtained values of C_{ij}, ν, and θ_D show that cubic $FAPbI_3$ is mechanically stable. The calculated value of B/G demonstrates that it has a ductile perovskite structure, easy bending, tensile and compressible. Our findings contribute to understanding the mechanism for photo-electrical performance of $FAPbI_3$ as a thin film absorber layer.

References

[1] National Renewable Energy Laboratory 2016

[2] Zhuang S W, Xu D Q, Xu J X, Wu B, Zhang Y T, Dong X, Li G X, Zhang B L and Du G T 2017 *Chin. Phys. B* **26** 017802

[3] Xie L, HWang H, Kim M and Kim K 2017 *Phys. Chem. Chem. Phys.* **197** 1143

[4] Kim H S, Lee C R, Im J H, Lee K B, Moehl T, Marchioro A, Moon S J, Humphry-Baker R, Yum J H, Moser J E, Gr?tzel M and Park N G 2012 *Sci. Rep.* **2** 591

[5] Baikie T, Fang Y, Kadro J M, Schreyer M, Wei F, Mhaisalkar S G, Grätzel M and White T J 2013 *J. Mater. Chem. A* **1** 5628

[6] Stoumpos C C, Malliakas C D and Kanatzidis G 2013 *Inorg. Chem.* **52** 9019

[7] Koh T M, Fu K, Fang Y, Chen S, Sum T C, Mathews N, Mhaisalkar S G, Boix P P and Baikie T 2014 *J. Phys. Chem. C* **118** 16458

[8] Eperon G E, Stranks S D, Menelaou C, Johnston M B, Herz L M and Snaith H J 2014 *Energy Environ. Sci.* **7** 982

[9] Pang S, Hu H, Zhang J, Lv S, Yu Y, Wei F, Qin T, Xu H, Liu Z and Cui G 2014 *Chem. Mater.* **26** 1485

[10] Maier M K and Gr?tzel M 2014 *Angew. Chem. Int. Ed.* **53** 3151

[11] Lee J W, Seol D J, Cho A N and Park N G 2014 *Adv. Mater.* **26** 4991

[12] Yang W S, Noh J H, Jeon N J, Kim Y C, Ryu S, Seo J and Seok S I 2015 *Science* **348** 1234

[13] Bi D, Tress W, Dar. M I, Gao P, Luo J, Renevier C, Schenk K, Abate A, Giordano F, Correa Baena J P, Decoppet J D, Zakeerudin S M, Nazeeruddin M K, Gra tzel M and Hagfeldt A 2016 *Science Adv.* **2** 2375

[14] Ma F H, Li J W, Li W Z, Lin N, Wang L D and Qiao J 2017 *Chem. Sci.* **8** 800

[15] Weller M T, Weber O J, Frost J M and Walsh A 2015 *J. Phys. Chem. Lett.* **6** 3209

[16] Kresse G and Hafner J 1993 *Phys. Rev. B* **47** 558

[17] Kresse G and Joubert D 1999 *Phys. Rev. B* **59** 1758

[18] Monkhorst H J and Pack J D 1976 *Phys. Rev. B* **13** 5188

[19] Perdew J P, Burke K and Ernzerhof M 1996 *Phys. Rev. Lett.* **77** 3865

[20] Tkatchenko A and Scheffler M 2009 *Phys. Rev. Lett.* **102** 073005

[21] Liu N, Wei Y, Ma X G, Zhu L, Xu G Wa, Chu L and Huang C Y 2017 *Acta Phys. Sin.* **66** 057103 (in Chinese)

[22] Motta C, Mellouhi F, Kais S, Tabet N, Harbi F H and Sanvito S 2015 *Nat. Commun.* **6** 7026

[23] Poglitsch A and Weber D 1987 *J. Chem. Phys.* **87** 6373

[24] Lang L, Yang J H, Liu H R, Xiang H J and Gong X G 2014 *Phys. Lett. A* **378** 290

[25] Dahani A, Alamri H, Merabet B, Zaoui A, Kacimi S, Boukortt A and Bejar M 2017 *Chin. Phys. B* **26** 017101

[26] Galkowski K, Mitioglu A, Miyata A, Plochocka P, Portugall O, Eperon G E, Tse J, Wang W, Stergiopoulos T, Stranks S D, Snaith H J and Nicholas R J 2016 *Energy Environ. Sci.* **9** 962

[27] Chang Y H, Park C H and Matsuishi K 2004 *J. Korean Phys. Soc.* **44** 889

[28] Lee J W, Kim H S and Park N G 2016 *Organic-Inorganic Halide Perovskite Photovoltaics* (Switzerland: Springer International Publishing) p. 223

[29] Eperona G E, Stranksa S D, Menelaoua C, Johnstona M B, Herza L M and Snaitha H J 2014 *Energy Environ. Sci.* **7** 982

[30] Bretschneider S A, Weickert J, Dorman J A and Schmidt-Mende L 2014 *APL Mater.* **2** 040701

[31] Mehl M J 1993 *Phys. Rev. B: Condens. Matter* **472** 493

[32] Niranjan M K 2012 *Intermetallics* **26** 150

[33] Zhang C M Jiang Y Yin D F Tao H J Sun S P and Yao J G 2016 *Acta Phys. Sin.* **65** 076101 (in Chinese)

[34] Fan T Zeng Q F and Yu S Y 2016 *Acta Phys. Sin.* **65** 118102 (in Chinese)

[35] Biskri Z, Rached H, Bouchear M and Rached D 2014 *J. Mech. Beh. Bio. Mater.* **32** 345.

[36] Pugh S F 1954 *Philos. Mag.* **45** 823

[37] Peng F, Chen D and Yang X D 2009 *Solid State Commun.* **149** 2135

[38] Feng J 2014 *APL Mater.* **2** 081801

[39] Wang J F, Fu X N, Zhang X D, Wang J T, Li X D and Jiang Z Y 2016 *Chin. Phys. B* **25** 086302

[40] Schreiber E, Anderson O and Soga N 1973 *Elastic Constants and their Measurements* (New York: McGraw-Hill)